Inorg. Chem. **1995,** *34,* 3801−3808

Mononuclear and Binuclear Molybdenum Complexes of the Tris(3,5-dimethyl-1-pyrazolyl)methane Ligand

Ish K. Dhawan, Michael A. Bruck, Brooke Schilling,[†] Carina Grittini, and John H. Enemark[*]

Department of Chemistry, University of Arizona, Tucson, Arizona 85721

Received January 26, 1995[⊗]

A series of mononuclear and binuclear molybdenum(0−VI) complexes of the facially coordinating tris(3,5-dimethyl-1-pyrazolyl)methane (L^*) ligand have been prepared and structurally and spectroscopically characterized. The oxidation of $L^*Mo(CO)_3$ by various oxidants such as $SOCl_2$, Br_2, I_2, and HNO_3 affords a variety of mononuclear molybdenum(III and VI) complexes of the type L^*MoX_3 (X = Cl, Br, I, and O). The synthesis of $[L^*MoOCl_2]^+Cl^-$ was achieved by refluxing a solution of L^* and $MoCl_5$ in THF. Oxo−molybdenum(V) complexes of the type $[L^*MoOX_2]^+$ were rapidly generated in solution by the action of 1 equiv of the dianions of catechol, tetrachlorocatechol, and ethanedithiol on $[L^*MoOCl_2]^+Cl^-$ in the presence of base. Upon standing, these reaction mixtures produce unsymmetrical dimers having a $[Mo_2O_4]^{2+}$ core. The structures of L^*MoI_3, $L^*Mo_2O_4Cl_2$, and $L^*Mo_2O_4(OC_6H_4O)$ were determined by X-ray crystallography: L^*MoI_3 crystallizes in the monoclinic space group $P2_1/n$ with $a = 15.756(1)$ Å, $b = 9.971(1)$ Å, $c = 16.822(1)$ Å, $\beta = 102.752(6)°$, $Z = 4$, $R = 0.024$, and $R_w = 0.036$. The molecule adopts the expected *fac* stereochemistry, and the average Mo−N and Mo−I distances are 2.200(3) and 2.7668(5) Å, respectively. $L^*Mo_2O_4Cl_2$ crystallizes in the orthorhombic space group *Pbca* with $a = 12.800(1)$ Å, $b = 18.530(1)$ Å, $c = 21.197(1)$ Å, $Z = 8$, $R = 0.034$, and $R_w = 0.047$. This binuclear complex contains both a six-coordinate molybdenum atom with an N_3O_3 coordination sphere and a five-coordinate molybdenum atom having O_3Cl_2 coordination. $L^*Mo_2O_4(OC_6H_4O)$ crystallizes in the orthorhombic space group $P2_12_12_1$ with $a = 7.979(1)$ Å, $b = 16.166(1)$ Å, $c = 21.767(3)$ Å, $Z = 4$, $R = 0.031$, and $R_w = 0.048$. This dimer is similar to the above mentioned binuclear complex except that chlorine atoms are replaced by the catecholate moiety. The ^{95}Mo NMR spectra of the dimeric species show a single peak that is assigned to the five-coordinate center.

Introduction

Facially coordinating tridentate nitrogen donor ligands are of current interest in bioinorganic chemistry because of their ability to mimic the tris(imidazole) binding sites of enzymes, provide protected binding pockets for small molecules, and control the nuclearity and reactivity pathways of metal centers.[1−3] The coordination chemistry of tris(3,5-dimethyl-1-pyrazolyl)borate[4] (L) and 1,4,7-triazacyclononane[5] (L′) ligands has been extensively developed during the past several years. However, the related neutral ligand tris(3,5-dimethyl-1-pyrazolyl)methane (L^*) (Figure 1) has been little studied since the initial synthesis of L^*, and a few metal complexes were first reported by Trofimenko[6] in 1970. Recently, a much improved synthesis of L^* was developed by Avila and co-workers[7] that gives up to 60% yield of high-purity L^*. This new procedure opens up the coordination chemistry of L^* with various metals and enables metal complexes of L^* to be compared to the extensively studied complexes of L and L′. Here we report the syntheses, X-ray structure determinations, spectroscopic characterizations, and chemical reactivities of several mononuclear and binuclear molybdenum complexes of L^* and compare the molybdenum chemistry of L^* to that of the tris(3,5-dimethyl-1-pyrazolyl)borate (L) and N-alkylated triazacyclononane (L′) ligands. The major difference in the chemistries of the molybdenum complexes of these ligands is that the oxo−Mo(V) complexes of L^* are much more labile than the corresponding complexes of L and L′.

Experimental Section

Reactions were carried out under an atmosphere of pure argon; solvents were thoroughly degassed before use. Solvents were purified by distillation: tetrahydrofuran from sodium benzophenone; acetonitrile from calcium hydride; chloroform from anhydrous calcium chloride. Anhydrous *N,N*-dimethylformamide was obtained from Aldrich Chemical Co. and used as received. Tris(3,5-dimethyl-1-pyrazolyl)methane[7] (L^*) was prepared by the literature method. Molybdenum pentachloride was obtained from Aldrich Chemical Co. Elemental analyses were performed by Desert Analytics, Tucson, AZ.

Preparation of Complexes. $L^*Mo(CO)_3$. The synthesis of $L^*Mo(CO)_3$ followed the literature method.[6] A solution of $Mo(CO)_6$ (0.25 g, 0.94 mmol) and L^* (0.3 g, 1.0 mmol) was heated (100−110 °C) in dry DMF for 8 h under an argon atmosphere. The yellow precipitate was collected by filtration, washed with ether, and air-dried; yield 0.34 g (70%). Anal. Calcd for $C_{19}H_{22}N_6O_3Mo$: C, 47.69; H, 4.60; N, 17.58. Found: C, 47.92; H, 4.60; N, 17.58.

L^*MoCl_3. $L^*Mo(CO)_3$ (0.25 mmol, 0.12 g) was suspended in 10 mL of $CHCl_3$ under an argon atmosphere, and $SOCl_2$ (2 mL) was added dropwise with stirring. The suspension was refluxed for approximately 6 h, and the yellow precipitate removed by filtration, washed with $CHCl_3$ and ether, and air-dried; yield 0.1 g (80%). The complex is soluble in DMF, DMSO, and CH_3CN and was recrystallized from CH_3CN. Anal. Calcd for $C_{16}H_{22}N_6Cl_3Mo$: C, 38.36; H, 4.39; N, 16.78. Found: C, 38.58; H, 4.30; N, 16.80.

L^*MoBr_3. $L^*Mo(CO)_3$ (0.25 mmol, 0.12 g) was suspended in 10 mL of $CHCl_3$ under an argon atmosphere, and Br_2 (0.5 mmol, 28 μL) dissolved in $CHCl_3$ was added dropwise with stirring to the reaction

---

[*] Author to whom correspondence should be addressed.

[†] Summer NSF-REU participant.

[⊗] Abstract published in *Advance ACS Abstracts,* June 1, 1995.

(1) Enemark, J. H.; Young, C. G. *Adv. Inorg. Chem.* **1993,** *40,* 1.

(2) Feig, A. L.; Lippard, S. J. *Chem. Rev.* **1994,** *94,* 759.

(3) Kitajima, N.; Moro-oka, Y. *Chem. Rev.* **1994,** *94,* 737.

(4) Trofimenko, S. *Chem. Rev.* **1993,** *93,* 943.

(5) Chaudhuri, P.; Wieghardt, K. *Prog. Inorg. Chem.* **1987,** *35,* 329.

(6) Trofimenko, S. *J. Am. Chem. Soc.* **1970,** *92,* 5118.

(7) Julia, S.; del Mazo, J. M.; Avila, L.; Elguero, J. *Org. Prep. Proceed. Int.* **1984,** *16,* 299.

0020-1669/95/1334-3801$09.00/0

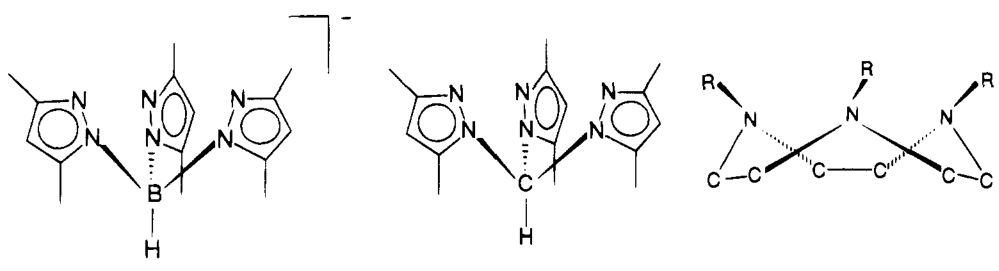

L **L*** **L'**

Figure 1. Structures of the facially coordinating tridentate ligands discussed in this paper: L, hydrotris(3,5-dimethyl-1-pyrazolyl)borate; L*, tris(3,5-dimethyl-1-pyrazolyl)methane; L′, 1,4,7-trialkyl-1,4,7-triazacyclonane (R = methyl unless otherwise specified).

mixture. The suspension was refluxed for approximately 10 h, and the deep yellow precipitate was removed by filtration, washed with $CHCl_3$ and ether, and air-dried; yield 0.14 g) 90%. The complex is soluble in DMF, DMSO, and CH_3CN and was recrystallized from CH_3CN. Anal. Calcd for $C_{16}H_{22}N_6Br_3Mo$: C, 30.29; H, 3.47; N, 13.25. Found: C, 30.32; H, 3.51; N, 13.28.

L^*MoI_3. A suspension of $L^*Mo(CO)_3$ (0.50 mmol, 0.24 g) and elemental iodine (0.25 mmol, 0.032 g) in 10 mL of concentrated HI was refluxed for 5 h. After cooling and addition of 5 mL of H_2O, the reaction mixture was again refluxed for 2 h. The orange precipitate was removed by filtration, washed with ethanol and ether, and air-dried; yield 0.35 g (90%). The complex is soluble in DMF, DMSO, and CH_3CN and was recrystallized from CH_3CN. Anal. Calcd for $C_{16}H_{22}N_6I_3Mo{\cdot}CH_3CN$: C, 26.47; H, 3.06; N, 12.00. Found: C, 26.21; H, 3.20, N, 12.00.

L^*MoO_3. $L^*Mo(CO)_3$ (0.25 mmol, 0.12 g) was added to 1 M HNO_3 (10 mL), and the reaction mixture was stirred in the presence of air for about 48 h. The white precipitate was removed by filtration, washed with water and ether, and air-dried; yield 0.04 g (40%). The complex is insoluble in all organic solvents.

$L^*Mo_2O_4Cl_2$. A solution of MoO_2Cl_2 (1.0 mmol, 0.2 g), PPh_3 (1.0 mmol, 0.26 g) and L* (1.0 mmol, 0.32 g) in dry DMF was stirred overnight at room temperature. An orange precipitate formed and was removed by filtration, washed with acetone and ether, and air-dried; yield 50%. Suitable X-ray-quality crystals were obtained by slow evaporation of a CH_3CN solution. This complex can be alternatively obtained by heating a solution of L* (0.5 mmol, 0.15 g) and $MoCl_4(CH_3CN)_2$ (0.2 mmol, 0.08 g) to 50° in THF (6 mL) for 3 h in the presence of a slight excess of degassed water (4 or 5 drops).

$[L^*MoOCl_2]^+Cl^-$. To $MoCl_5$ (2 mmol, 0.55 g) in a 100 mL Schlenk flask at −77 °C was slowly added 50 mL of THF with vigorous stirring. The reaction mixture was gradually brought to room temperature with continuous stirring. Near room temperature the color of the reaction mixture changed from dark red-brown to green. To the green solution, under argon atmosphere, was added L* (2 mmol, 0.60 g), and the mixture was heated to 50 °C for 12 h with stirring. The resultant green precipitate was filtered off under an argon atmosphere and washed with a small amount of THF; yield 0.6 g (58%). The product is very air and moisture sensitive and tends to form dimers. Suitable elemental analysis results could not be obtained because the complex was always contaminated with trace amounts of dimers.

$L^*Mo_2O_4(OC_6H_4O)$. To a solution of $[L^*MoOCl_2]^+Cl^-$ (0.25 mmol, 0.13 g) and HOC_6H_4OH (0.3 mmol, 0.036 g) in 15 mL of acetonitrile was added Et_3N (0.5 mmol, 100 μL) dropwise with stirring. The reaction mixture turned deep green immediately. After a few days the reaction mixture became purple, and purple crystals deposited at the bottom of the flask. The crystals were washed with ether and acetonitrile and air-dried; yield 35%.

Physical Measurements. Infrared spectra were obtained in KBr pellets and in solution IR cells on a Perkin-Elmer PE983 spectrometer. Optical spectra were recorded on an On-Line Instrument Systems (OLIS) 4300S modified Cary 14 spectrometer using quartz cells (1.0 cm path length). EPR spectra on either fluid solutions or frozen glasses were obtained with a Bruker ESP 300E spectrometer operating at X-band (ca. 9.1 GHz). Frequencies were measured with a Systron Donner-6530 frequency counter. Liquid nitrogen temperature was maintained using a quartz immersion Dewar flask. Simulation of the frozen solution EPR spectrum was done using a modified version of the program QPOW written by Prof. R. L. Belford and co-workers.[8] The $I = {}^5/_2$ (^{95,97}Mo isotopes, 25% abundant) and $I = 0$ (^{92,94,96,98}Mo isotopes, 75% abundant) components were simulated separately and then summed to obtain the complete spectrum. Cyclic voltammograms were recorded on a BAS CV-50W system at 100−150 mV/s in acetonitrile solutions (1−2 mM). The reference electrode was silver/silver chloride, a BAS Model MF-2063 platinum electrode was used as the working electrode, and a platinum wire served as the counter electrode. The supporting electrolyte was a 0.1 M solution of tetramethylammonium hexafluorophosphate in acetonitrile. All half-wave potentials were internally referenced against the ferrocenium/ferrocene (Fc^+/Fc) couple. ^{95}Mo NMR spectra were recorded on a Bruker AM250 spectrometer.[9] Chemical shifts were referenced to external 2 M Na_2MoO_4 solution in D_2O (pH = 11).

Structure Determinations. Crystal data are summarized in Table 1. Full details of the structure determinations are given in the supporting information. All intensity data were collected on an Enraf-Nonius CAD4 diffractometer using Mo Kα radiation (λ = 0.710 73 Å). Scattering factors were taken from Cromer and Waber;[10] anomalous dispersion effects were included for all non-hydrogen atoms with the values of $\Delta f'$ and $\Delta f''$ taken from Cromer.[11] All calculations were performed on a VAX using MolEN (Enraf-Nonius) and SHELXS-86,[12] and the least-squares refinements minimized $\sum w(|F_o| - |F_c|)^2$, with $w = 4F_o^2/\sigma^2(F_o^2)$.

Results and Discussion

Syntheses. The syntheses of various mononuclear molybdenum(0, III, and VI) complexes of the neutral tridentate tris(3,5-dimethyl-1-pyrazolyl)methane (L*) ligand are summarized in Scheme 1. Prolonged refluxing of $L^*Mo(CO)_3$ with the appropriate halogenating agent leads to oxidation−decarbonylation reactions and formation of molybdenum(III) complexes of the type L^*MoX_3 (X= Cl, Br, I). These complexes are air stable and soluble in polar organic solvents (DMSO, DMF, acetonitrile). The monomeric nature of the L^*MoX_3 complexes was proven by the determination of the structure of $LMoI_3$ (Figure 2) (vide infra). Exhaustive oxidation of $L^*Mo(CO)_3$ with nitric acid yields the colorless molybdenum(VI) complex L^*MoO_3, which is insoluble in all common organic solvents. This complex shows oxo−molybdenum stretching frequencies similar to those reported for $L'MoO_3$ (R = isopropyl).[13] The

---

(8) (a) Belford, R. L.; Nilges, M. J. Computer Simulation of Powder Spectra. Paper presented at the EPR Symposium, 21st Rocky Mountain Conference, Denver, Aug 1979. (b) Nilges, M. J. Ph.D. Dissertation, University of Illinois, Urbana, IL, 1979.

(9) Minelli, M.; Young, C. G.; Enemark, J. H. *Inorg. Chem.*. **1985,** *24,* 1111.

(10) Cromer, D. T.; Waber, J. T. In *International Tables for X-Ray Crystallography*; Kynoch: Birmingham, England, 1974; Vol. IV, Table 2.2B.

(11) Cromer, D. T. In *International Tables for X-Ray Crystallography;* Kynoch: Birmingham, England, 1974; Vol. IV, Table 2.3.1.

(12) Sheldrick, G. M. *Acta Crystallogr.* **1990,** *A46,* 467.

(13) Haselhorst, G.; Stoetzel, S.; Strassburger, A.; Walz, W.; Wieghardt, K.; Nuber, B. *J. Chem. Soc., Dalton Trans.* **1993,** 83.

Table 1. Summary of Crystal Data

	L*MoI$_3$	L*Mo$_2$O$_4$Cl$_2$	L*Mo$_2$O$_4$(OC$_6$H$_4$O)
formula	I$_3$MoN$_6$C$_{16}$H$_{22}$·CH$_3$CN	Mo$_2$Cl$_2$O$_4$N$_6$C$_{16}$H$_{22}$·CH$_3$CN	Mo$_2$O$_6$N$_6$C$_{22}$H$_{26}$·CH$_3$CN
fw	816.10	663.23	703.42
crystal dimensions (mm)	0.10 × 0.25 × 0.60	0.33 × 0.33 × 0.33	0.25 × 0.33 × 0.50
temp (°C)	21 ± 1	20 ± 1	21 ± 1
crystal class	monoclinic	orthorhombic	orthorhombic
space group	*P*2$_1$/*n*	*Pbca*	*P*2$_1$2$_1$2$_1$
cell parameters			
a (Å)	15.756(1)	12.800(1)	7.979(1)
b (Å)	9.971(1)	18.530(1)	16.166(1)
c (Å)	16.822(1)	21.197(1)	21.767(3)
β (Å)	102.752(6)		
V (Å)	2577.3(6)	5027.6(6)	2807.7(4)
Z (Å)	4	8	4
calcd density (g/cm^3)	2.10	1.76	1.66
ab coeff (g/cm^{-1})	40.7	12.3	9.1
no of reflections included	3833 with $F_o^2 > 3.0\sigma(F_o^2)$	3332 with $F_o^2 > 3.0\sigma(F_o^2)$	2663 with $F_o^2 > 3.0\sigma(F_o^2)$
no of parameters refined	262	298	352
unweighted agreement factor	0.024	0.034	0.031
weighted agreement factor	0.036	0.047	0.048
esd of observn of unit weight	1.33	1.57	1.88

Scheme 1

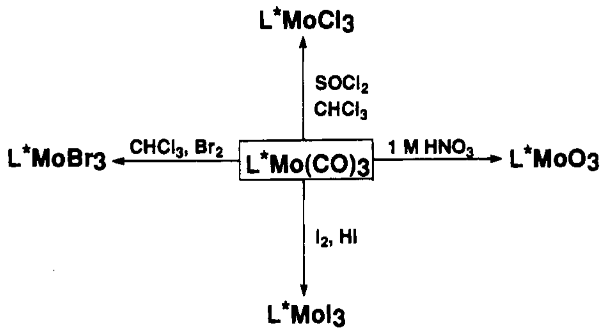

molybdenum(0, III, and VI) compounds of L* in Scheme 1 parallel the analogous molybdenum complexes of L′.[14]

The cationic monooxo–molybdenum(V) complex [L*MoOCl$_2$]$^+$Cl$^-$ is accessible by the synthetic route used to prepare LMoOCl$_2$.[15] The product has UV-vis, IR, and EPR spectra similar to those of LMoOCl$_2$,[15] but [L*MoOCl$_2$]$^+$Cl$^-$ and LMoOCl$_2$ exhibit very different chemical properties. LMoOCl$_2$ is indefinitely stable in solution, and substitution reactions of the Cl$^-$ ligands require prolonged refluxing times. However, [L*MoOCl$_2$]$^+$Cl$^-$ is air and moisture sensitive; substitution reactions are facile and proceed readily at room temperature. Reaction of [L*MoOCl$_2$]$^+$Cl$^-$ with catechol, tetrachlorocatechol, or 1 equiv of ethanedithiol in acetonitrile in the presence of base initially forms mononuclear monooxo–molybdenum(V) complexes in solution of the type [L*MoOX$_2$]$^-$ (X$_2$ = dianion of catechol, tetrachlorocatechol, or ethanedithiol) as shown in Scheme 2. The formulation of these compounds is based upon the similarity of their EPR spectral parameters (vide infra) to the well-known mononuclear monooxo–molybdenum(V) complexes of the type LMoOX$_2$.[15,16,17]

Addition of ≥2 equiv of ethanedithiol to [L*MoOCl$_2$]$^+$Cl$^-$ leads to the formation of [MoO(SCH$_2$CH$_2$S)$_2$]$^-$, which was identified by comparison of its EPR spectrum to that of an authentic sample synthesized independently.[18] The formation of [MoO(SCH$_2$CH$_2$)$_2$]$^-$ in the presence of excess ethanedithiol implies that the neutral bulky L* ligand is quite labile. This substitution behavior contrasts with that of the anionic L ligand, which remains coordinated to LMoOXY complexes even at elevated temperatures.

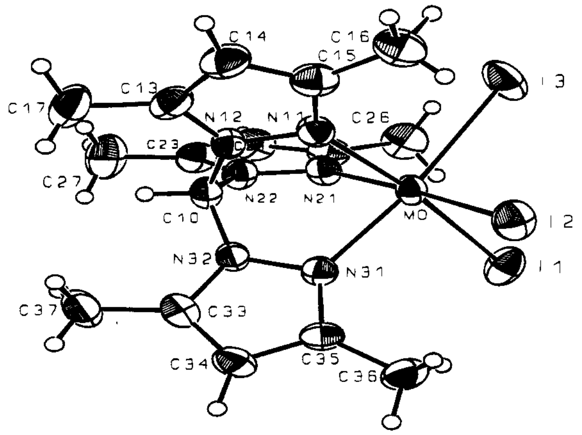

Figure 2. ORTEP drawing of L*MoI$_3$. The atoms are drawn as 50% probability ellipsoids, and H atom radii have been reduced for clarity.

Initial attempts to synthesize L*Mo^{IV}OCl$_2$ by reaction of MoO$_2$Cl$_2$ with PPh$_3$ yielded an orange complex, which was later characterized by X-ray diffraction to be the unsymmetrical dimer L*Mo$_2$O$_4$Cl$_2$ (Figure 3) having a [Mo$_2$O$_4$]$^{2+}$ core. This product was also isolated when the reaction mixtures of Scheme 2 were allowed to stand for several hours. This facile formation of binuclear complexes precluded isolation of the monomeric oxo–molybdenum(V) species from the reaction mixtures in Scheme 2. The unsymmetrical dimer [L*Mo$_2$O$_4$(OC$_6$H$_4$O)] (Figure 4) was isolated from the reaction mixture of catechol and [L*MoOCl$_2$]$^+$Cl$^-$ in CH$_3$CN in the presence of Et$_3$N. The pathway for the formation of these unsymmetrical dimers is not yet understood, but the lability of the ligand (L*) is likely one of the reasons for the formation of these complexes possessing the thermodynamically stable [Mo$_2$O$_4$]$^{2+}$ core.

Structure Determinations. To our knowledge, there are no prior reports of structural studies of metal complexes of L*. However, several bis(ligand) complexes of the parent tris(pyrazolyl)methane ligand (no methyl groups) with first-row transition metals have been structurally characterized.[19,20] Each

---

(14) Backes-Dahmann, G.; Herrmann, W.; Wieghardt, K.; Weiss, J. *Inorg. Chem.* **1985,** *24,* 485.

(15) Cleland, W. E., Jr.; Barnhart, K. M.; Yamanouchi, K.; Collison, D.; Mabbs, F. E.; Ortega, R. B.; Enemark, J. H. *Inorg. Chem.* **1987,** *26,* 1017.

(16) Dhawan, I. K.; Pacheco, A.; Enemark, J. H. *J. Am. Chem. Soc.* **1994,** *116,* 7911.

(17) Basu, P.; Bruck, M. A.; Li, Z.; Dhawan, I. K.; Enemark, J. H. *Inorg. Chem.*, in press.

(18) Ellis, S. R.; Collison, D.; Garner, C. D.; Clegg, W. *J. Chem. Soc., Chem. Commun.* **1986,** 1483.

Scheme 2

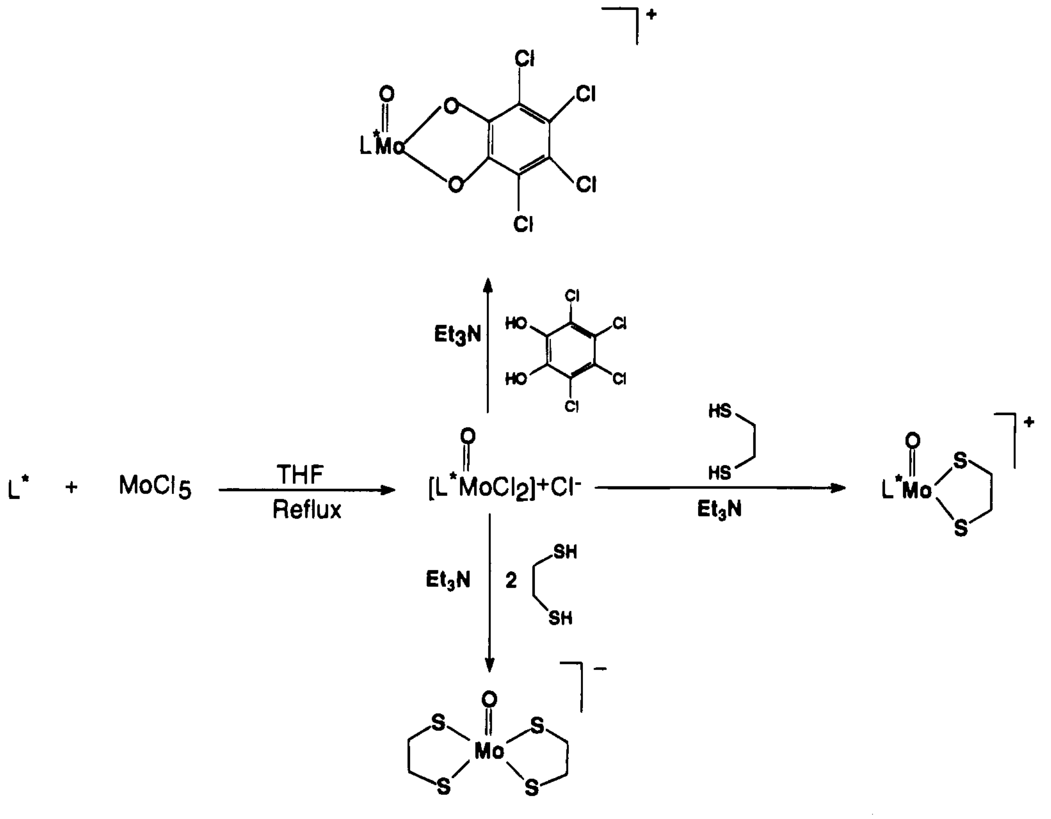

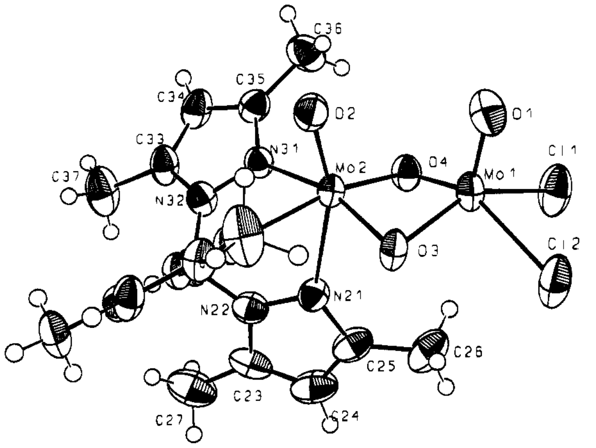

Figure 3. ORTEP drawing of $L^*Mo_2O_4Cl_2$. The atoms are drawn as 50% probability ellipsoids, and H atom radii have been reduced for clarity.

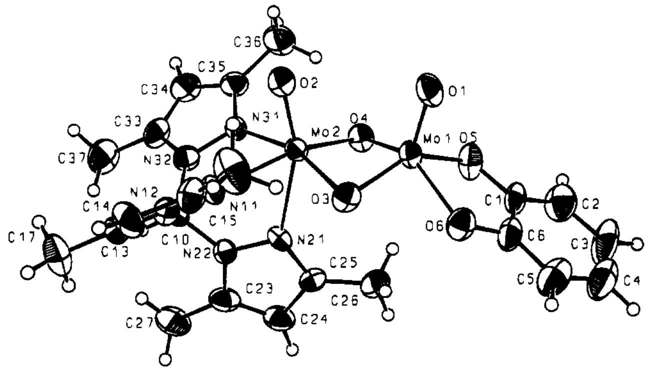

Figure 4. ORTEP drawing of $L^*Mo_2O_4(OC_6H_4O)$. The atoms are drawn as 50% probability ellipsoids, and H atom radii have been reduced for clarity.

of the compounds investigated (Table 1) crystallizes with one well-ordered solvent molecule of CH_3CN per molecule of complex.

L^*MoI_3. The structure of L^*MoI_3 determined by single crystal X-ray diffraction is shown in Figure 2. The coordination of the molybdenum(III) center is pseudooctahedral with the neutral tridentate tris(3,5-dimethyl-1-pyrazolyl)methane (L*) bonding facially and the other three sites occupied by iodine ligands. The local symmetry around the molybdenum center is approximately C_{3v}. Positional parameters and selected bond distances and angles are shown in Tables 3 and 4, respectively. The low solubility of $L^*Mo(CO)_3$ thwarted all attempts to grow diffraction-quality crystals for direct structural comparison to $[LMo(CO)_3]^-$, but the structural similarities between L and L* are apparent from comparison of the average distances and angles for $[Et_4N][LMo(CO)_3]$[21] and L^*MoI_3. The major difference between the two systems is that the B−N distance of L is ~0.1 Å longer than the corresponding C−N distance of L*. The average Mo−N distance in $L^*Mo^{III}I_3$ (2.200 Å) is similar to that in the preliminary report of the structure of $[LMo^{III}Cl_3]^-$.[22]

$L^*Mo_2O_4Cl_2$. The binuclear structure of $L^*Mo_2O_4Cl_2$ is unusual in that it exhibits two distinctly different oxo−molybdenum centers (Figure 3). Mo1 is five-coordinate with square pyramidal coordination, one terminal oxo ligand, two equatorial oxo bridges to Mo2, and two equatorial terminal chlorine atoms. The sixth coordination site of Mo1 is blocked by a methyl group (Mo1−C26 = 3.572 Å) from the L* ligand coordinated to Mo2. The five-coordinate Mo1 center has Mo1−O1 = 1.655(4) Å. The oxygen atoms bridging to Mo2 are at distances of 1.930-

---

(19) Astley, T.; Gulbis, J. M.; Hitchman, M. A.; Tiekink, E. R. T. *J. Chem. Soc., Dalton Trans.* **1993,** 509.

(20) Canty, A. J.; Minchin, N. J.; Engelhardt, L. M.; Skelton, B. W.; White, A. H. *J. Chem. Soc., Dalton Trans.* **1986,** 645.

(21) Marabella, C. P.; Enemark, J. H. *J. Organomet. Chem.* **1982,** *226,* 57.

(22) Millar, M.; Lincoln, S. H. C. J.; Koch, S. A. *J. Am. Chem. Soc.* **1982,** *104,* 288.

Table 2. Positional Parameters and Their Estimated Standard Deviations for $L^*MoI_3{\cdot}CH_3CN$

atom	*x*	*y*	*z*	B^a (Å^2)
Mo	0.53957(2)	0.29562(3)	0.29836(2)	2.433(6)
I1	0.66196(2)	0.11004(3)	0.27324(2)	4.020(6)
I2	0.40298(2)	0.16388(3)	0.19555(2)	3.744(6)
I3	0.51065(2)	0.16967(3)	0.43560(2)	4.767(7)
N11	0.4536(2)	0.4636(3)	0.3147(2)	2.86(7)
N12	0.4841(2)	0.5901(3)	0.3071(2)	2.61(6)
C13	0.4275(3)	0.6848(4)	0.3196(3)	3.46(9)
C14	0.3582(3)	0.6169(5)	0.3350(3)	4.1(1)
C15	0.3755(3)	0.4825(5)	0.3322(3)	3.58(9)
C16	0.3171(3)	0.3704(6)	0.3451(3)	5.0(1)
C17	0.4439(4)	0.8333(5)	0.3146(4)	5.1(1)
N21	0.6414(2)	0.4235(3)	0.3715(2)	2.71(6)
N22	0.6366(2)	0.5575(3)	0.3545(2)	2.73(6)
C23	0.6980(3)	0.6287(4)	0.4064(3)	3.21(8)
C24	0.7450(3)	0.5350(5)	0.4575(3)	3.75(9)
C25	0.7087(3)	0.4113(5)	0.4354(2)	3.16(8)
C26	0.7366(3)	0.2814(5)	0.4761(3)	4.4(1)
C27	0.7058(3)	0.7759(5)	0.4019(4)	5.0(1)
N31	0.5628(2)	0.4207(3)	0.1976(2)	2.53(6)
N32	0.5734(2)	0.5555(3)	0.2124(2)	2.48(6)
C33	0.5843(3)	0.6232(4)	0.1453(3)	3.00(8)
C34	0.5837(3)	0.5304(4)	0.0866(2)	3.22(8)
C35	0.5682(2)	0.4045(4)	0.1194(2)	2.82(8)
C36	0.5597(3)	0.2748(5)	0.0765(3)	4.0(1)
C37	0.5948(3)	0.7724(5)	0.1442(3)	4.2(1)
C10	0.5685(2)	0.6094(4)	0.2893(2)	2.65(7)
N	0.3704(4)	0.6730(7)	0.1118(3)	7.9(2)
C1	0.3168(4)	0.5991(7)	0.1158(4)	5.8(1)
C2	0.2478(4)	0.5110(7)	0.1225(4)	6.9(2)

[a] Anisotropically refined atoms are given in the form of the isotropic equivalent displacement parameter defined as $(4/3)[a^2B(1,1) + b^2B(2,2) + c^2B(3,3) + ab(\cos\gamma)B(1,2) + ac(\cos\beta)B(1,3) + bc(\cos\alpha)B(2,3)]$.

Table 3. Selected Bond Distances (Å) and Angles (deg) in $L^*MoI_3{\cdot}CH_3CN$

	Distances		
Mo−I1	2.7714(5)	Mo−I2	2.7758(4)
Mo−I3	2.7532(5)	Mo−N11	2.209(3)
Mo−N21	2.200(3)	Mo−N31	2.199(3)
N11−N12	1.366(5)	N31−N32	1.371(5)
N21−N22	1.366(5)	N12−C10	1.440(5)
N22−C10	1.450(5)	N32−C10	1.418(5)
	Angles		
I1−Mo−I2	93.38(1)	I1−Mo−I3	94.17(2)
I1−Mo−N11	172.57(9)	I1−Mo−N21	91.51(9)
I1−Mo−N31	91.21(9)	I2−Mo−I3	93.30(1)
I2−Mo−N11	91.37(9)	I2−Mo−N21	172.72(9)
I2−Mo−N31	91.50(9)	I3−Mo−N11	91.25(9)
I3−Mo−N21	91.73(9)	I3−Mo−N31	172.56(9)
N11−Mo−N21	83.2(1)	N11−Mo−N31	82.9(1)
N21−Mo−N31	83.0(1)	Mo−N11−N12	116.8(2)
Mo−N31−N32	116.8(2)	N12−C10−N32	112.2(3)
N12−C10−N22	110.9(3)	N22−C10−N32	112.0(3)

(3) and 1.928(3) Å from Mo1 while Mo1−Cl1 and Mo1−Cl2 distances are 2.387(1) and 2.408(1) Å, respectively. The Mo2 atom has distorted octahedral coordination geometry, with the neutral tridentate ligand (L*) occupying one trigonal face. A terminal oxo ligand (Mo2−O2 = 1.668(3) Å) and two bridging oxo ligands (Mo2−O3 = 1.906(3) Å; Mo2−O4 = 1.912(3) Å) occupy the opposite face. The central $[Mo_2O_4]^{2+}$ unit exhibits syn stereochemistry, and the Mo−Mo distance of 2.563 Å is consistent with the known Mo−Mo distances of bis(*μ*-oxo) dimers.[23,24] The bond distances and angles involving L* are similar to those observed for L^*MoI_3. Positional parameters and selected bond distances and angles of $L^*Mo_2O_4Cl_2$ are given Tables 4 and 5, respectively.

Table 4. Positional Parameters and Their Estimated Standard Deviations for $L^*Mo_2O_4Cl_2{\cdot}CH_3CN$

atom	*x*	*y*	*z*	B^a (Å^2)
Mo1	0.22568(3)	0.18282(2)	0.11418(2)	2.984(8)
Mo2	0.22875(3)	0.14192(2)	−0.00133(2)	2.498(7)
Cl1	0.3655(1)	0.20364(9)	0.18645(6)	5.19(3)
Cl2	0.1385(1)	0.12981(9)	0.20352(6)	5.03(3)
O1	0.1679(3)	0.2625(2)	0.1086(2)	4.34(8)
O2	0.1697(3)	0.2131(2)	−0.0338(2)	3.63(7)
O3	0.1463(2)	0.1112(2)	0.0686(1)	3.08(6)
O4	0.3369(2)	0.1762(2)	0.0532(1)	3.06(6)
C	0.2998(3)	0.0168(3)	−0.1066(2)	3.2(1)
N11	0.1388(3)	0.0682(2)	−0.0644(2)	2.94(8)
N12	0.1873(3)	0.0228(2)	−0.1056(2)	2.86(7)
C13	0.1171(4)	−0.0170(2)	−0.1391(2)	3.1(1)
C14	0.0211(4)	0.0054(3)	−0.1192(2)	3.6(1)
C15	0.0365(3)	0.0577(3)	−0.0739(2)	3.3(1)
C16	−0.0433(4)	0.0994(3)	−0.0389(2)	4.9(1)
C17	0.1479(4)	−0.0705(3)	−0.1876(2)	4.5(1)
N21	0.3124(3)	0.0269(2)	0.0067(2)	3.10(8)
N22	0.3366(3)	−0.0098(2)	−0.0471(2)	3.36(8)
C23	0.3837(4)	−0.0743(3)	−0.0350(3)	4.1(1)
C24	0.3888(4)	−0.0779(3)	0.0287(3)	5.0(1)
C25	0.3453(4)	−0.0152(3)	0.0530(2)	3.9(1)
C26	0.3328(5)	0.0050(3)	0.1210(2)	5.5(1)
C27	0.4147(5)	−0.1258(3)	−0.0847(3)	5.8(2)
N31	0.3432(3)	0.1407(2)	−0.0799(2)	2.76(7)
N32	0.3483(3)	0.0849(2)	−0.1214(2)	3.05(8)
C33	0.4079(4)	0.1023(3)	−0.1723(2)	3.8(1)
C34	0.4416(4)	0.1704(3)	−0.1621(2)	4.0(1)
C35	0.4000(4)	0.1938(3)	−0.1050(2)	3.2(1)
C36	0.4134(4)	0.2639(3)	−0.0733(3)	4.6(1)
C37	0.4251(4)	0.0521(3)	−0.2260(2)	5.6(1)
N1	0.1800(5)	0.3943(3)	0.2526(3)	7.2(1)
C1	0.1645(5)	0.3419(3)	0.2769(3)	4.7(1)
C2	0.1487(6)	0.2752(3)	0.3099(3)	7.4(2)

[a] Anisotropically refined atoms are given in the form of the isotropic equivalent displacement parameter defined as $(4/3)[a^2B(1,1) + b^2B(2,2) + c^2B(3,3) + ab(\cos\gamma)B(1,2) + ac(\cos\beta)B(1,3) + bc(\cos\alpha)B(2,3)]$.

$L^*Mo_2O_4(OC_6H_4O)$. The molecular structure of $L^*Mo_2O_4(OC_6H_4O)$ is shown in Figure 4; positional parameters and selected distances and angles appear in Tables 6 and 7, respectively. This dinuclear complex is structurally similar to $L^*Mo_2O_4Cl_2$ (Figure 3) with the two terminal chlorine atoms replaced by a catecholate moiety. The Mo1−O(catechol) distances are 2.013(5) and 2.006(5) Å, slightly longer than the average Mo−O(catechol) distance of 1.986(3) Å in the mononuclear six-coordinate $LMoO(catCl_4)$ complex.[17] The average Mo1−O(catechol) length of $L^*Mo_2O_4(OC_6H_4O)$ falls within the range of Mo(VI)−O lengths (2.014(5)−1.956(5) Å) for structurally characterized mononuclear mono-oxo Mo(VI)(cat) complexes.[25,26] The coordination geometry and bond distances and angles of Mo2 are nearly identical to those of Mo2 in $L^*Mo_2O_4Cl_2$.

Spectroscopy. ^{95}Mo NMR. Complexes $L^*Mo_2O_4Cl_2$ and $L^*Mo_2O_4(OC_6H_4O)$ are diamagnetic in solution and exhibit single ^{95}Mo resonances at δ 565 and 124, respectively. The line widths observed for these complexes are 320 and 100 Hz, respectively. Observation of ^{95}Mo NMR signals depends on various factors,[27] and ^{95}Mo NMR data on a wide variety of

---

(23) Garner, C. D.; Charnock, J. M. In *Comprehensive Coordination Chemistry;* Wilkinson, G., Gillard, R. D., McCleverty, J. A., Eds.; Pergamon Press: New York, 1985; Vol. 3, pp 1329−1375.

(24) Stiefel, E. I. *Prog. Inorg. Chem.* **1977,** *22,* 1.

(25) (a) Bristow, S.; Enemark, J. H.; Garner, C. D.; Minelli, M.; Morris, G. A.; Ortega, R. B. *Inorg. Chem.* **1985,** *24,* 4070. (b) Bristow, S.; Garner, C. D.; Morris, G. A.; Minelli, M.; Enemark, J. H.; Ortega, R. B. *Polyhedron* **1986,** *5,* 319.

(26) Mondal, J. U.; Schultz, F. A.; Brennan, T. D.; Scheidt, W. R *Inorg. Chem.* *1988,* 27, 3950.

Table 5. Selected Bond Distances (Å) and Angles (deg) in $L^*Mo_2O_4Cl_2 \cdot CH_3CN$

	Distance		
Mo1−Mo2	2.5633(5)	Mo1−Cl1	2.387(1)
Mo1−Cl2	2.408(1)	Mo1−O1	1.655(4)
Mo1−O3	1.930(3)	Mo1−O4	1.928(3)
Mo2−O2	1.668(3)	Mo2−O3	1.906(3)
Mo2−O4	1.912(3)	Mo2−N11	2.232(4)
Mo2−N21	2.391(4)	Mo2−N31	2.217(4)
C−N12	1.446(6)	C−N22	1.433(6)
C−N32	1.440(6)	N11−N12	1.363(5)
N21−N22	1.364(5)	N31−N32	1.360(5)
	Angles		
Mo2−Mo1−Cl1	130.49(4)	O2−Mo2−N31	89.9(2)
Mo2−Mo1−Cl2	129.63(4)	O3−Mo2−O4	91.8(1)
Mo2−Mo1−O1	101.7(1)	O3−Mo2−N11	89.8(1)
Mo2−Mo1−O3	47.67(9)	O3−Mo2−N21	85.8(1)
Mo2−Mo1−O4	47.86(9)	O3−Mo2−N31	161.1(1)
Cl1−Mo1−Cl2	84.76(5)	O4−Mo2−N11	159.9(1)
Cl1−Mo1−O1	103.7(1)	O4−Mo2−N21	85.9(1)
Cl1−Mo1−O3	145.8(1)	O4−Mo2−N31	88.8(1)
Cl1−Mo1−O4	83.5(1)	N11−Mo2−N21	74.2(1)
Cl2−Mo1−O1	102.3(1)	N11−Mo2−N31	83.4(1)
Cl2−Mo1−O3	82.5(1)	N21−Mo2−N31	75.4(1)
Cl2−Mo1−O4	147.6(1)	Mo1−O3−Mo2	83.8(1)
O1−Mo1−O3	110.0(2)	Mo1−O4−Mo2	83.8(1)
O1−Mo1−O4	109.8(2)	N12−C−N22	110.0(4)
O3−Mo1−O4	90.5(1)	N12−C−N32	111.4(4)
Mo1−Mo2−O2	98.8(1)	N22−C−N32	110.5(4)
Mo1−Mo2−O3	48.48(9)	Mo1−Mo2−O4	48.38(9)
Mo1−Mo2−N11	138.2(1)	Mo1−Mo2−N21	101.68(9)
C−N12−N11	120.7(4)	Mo1−Mo2−N31	136.9(1)
C−N12−C13	127.5(4)	O2−Mo2−O3	107.8(2)
O2−Mo2−O4	108.3(2)	O2−Mo2−N11	90.2(2)
O2−Mo2−N21	159.5(1)		

Table 6. Positional Parameters and Their Estimated Standard Deviations for $L^*Mo_2O_4(OC_6H_4O) \cdot CH_3CN$

atom	x	y	z	B^a (Å^2)
Mo1	0.15927(7)	0.46571(3)	0.64422(2)	2.479(9)
Mo2	0.10190(6)	0.31718(3)	0.67958(2)	2.142(8)
O1	0.0797(7)	0.5249(3)	0.7010(2)	3.7(1)
O2	−0.0008(7)	0.3369(3)	0.7455(2)	3.50(9)
O3	0.3029(5)	0.3829(3)	0.6791(2)	2.95(8)
O4	0.0003(6)	0.3851(3)	0.6161(2)	2.67(8)
O5	0.0936(7)	0.5238(3)	0.5660(2)	3.8(1)
O6	0.3797(6)	0.5142(3)	0.6183(2)	3.46(9)
N11	0.2435(7)	0.2162(3)	0.7249(2)	2.6(1)
N12	0.2340(7)	0.1353(3)	0.7065(2)	2.6(1)
N21	0.2261(7)	0.2407(3)	0.5972(2)	2.6(1)
N22	0.2215(7)	0.1563(3)	0.5990(2)	2.6(1)
N31	−0.0784(7)	0.2162(3)	0.6572(2)	2.6(1)
N32	−0.0300(7)	0.1352(3)	0.6543(2)	2.7(1)
C1	0.215(1)	0.5735(4)	0.5414(3)	3.1(1)
C2	0.189(1)	0.6255(5)	0.4939(3)	5.0(2)
C3	0.325(2)	0.6745(5)	0.4741(4)	6.3(2)
C4	0.479(1)	0.6658(5)	0.5002(4)	5.7(2)
C5	0.507(1)	0.6111(5)	0.5488(3)	4.8(2)
C6	0.372(1)	0.5654(4)	0.5696(3)	3.6(1)
C10	0.1456(8)	0.1146(4)	0.6507(3)	2.6(1)
C13	0.3218(9)	0.0858(4)	0.7449(3)	2.9(1)
C14	0.386(1)	0.1354(5)	0.7895(3)	3.9(1)
C15	0.339(1)	0.2162(4)	0.7749(3)	3.3(1)
C16	0.370(1)	0.2944(5)	0.8097(3)	5.0(2)
C17	0.333(1)	−0.0068(4)	0.7377(4)	5.2(2)
C23	0.290(1)	0.1221(4)	0.5471(3)	3.5(1)
C24	0.343(1)	0.1866(4)	0.5118(3)	3.6(1)
C25	0.3004(8)	0.2594(4)	0.5441(3)	2.5(1)
C26	0.334(1)	0.3438(4)	0.5233(3)	3.9(1)
C27	0.297(1)	0.0318(4)	0.5363(4)	5.3(2)
C33	−0.1637(9)	0.0853(4)	0.6485(3)	3.4(1)
C34	−0.2993(9)	0.1343(4)	0.6486(3)	3.8(1)
C35	−0.2451(8)	0.2155(4)	0.6540(3)	3.1(1)
C36	−0.344(1)	0.2940(4)	0.6586(4)	4.8(2)
C37	−0.149(1)	−0.0072(4)	0.6431(4)	4.9(2)
N	0.241(1)	−0.1395(5)	0.6270(4)	7.7(2)
C51	0.189(1)	−0.2027(5)	0.6386(4)	5.5(2)
C52	0.135(2)	−0.2833(5)	0.6551(5)	8.1(3)

[a] Anisotropically refined atoms are given in the form of the isotropic equivalent displacement parameter defined as $(4/3)[a^2B(1,1) + b^2B(2,2) + c^2B(3,3) + ab(\cos\gamma)B(1,2) + ac(\cos\beta)B(1,3) + bc(\cos\alpha)B(2,3)]$.

mononuclear and polynuclear molybdenum complexes in various oxidation states have been tabulated.[28] Symmetrical binuclear Mo(V) complexes possessing the $[Mo_2O_4]^{2+}$ core often exhibit narrow line widths, but to the best of our knowledge, there are no ^{95}Mo NMR data available for unsymmetrical $[Mo_2O_4]^{2+}$ dimers. Observation of a single relatively sharp peak in the ^{95}Mo NMR spectrum for each of the dimers of Figures 3 and 4 indicates that only one of their two chemically inequivalent molybdenum atoms is detectable by ^{95}Mo NMR. From the substantial difference in chemical shift between the two molecules, the most reasonable assignment for the observed resonance is Mo1, whose coordinations differ in the two compounds. If each metal center obeys the electroneutrality principle,[29] then the Mo1 centers are formally Mo(VI), whereas the Mo2 centers are formally Mo(IV). Consistent with this view, oxo−Mo(VI) complexes are usually easily detectable by ^{95}Mo NMR and exhibit chemical shifts in the range observed here; oxo−Mo(IV) compounds are often difficult to detect by ^{95}Mo NMR because they typically exhibit very large line widths and consequently require high concentrations of sample (0.2−0.6 M) to be observed.[27] Thus, the ^{95}Mo NMR data favor describing these unsymmetrical diamagnetic dimers as possessing six-coordinate oxo−Mo(IV) and five-coordinate oxo−Mo(VI) centers.

Electronic Absorption. In acetonitrile solution the L^*MoX_3 (X = Cl, Br, I) complexes exhibit absorption maxima (Table 8) in agreement with other octahedral molybdenum(III) complexes with an $S = {}^3/_2$ ground state.[14,24] The electronic spectrum of $[L^*MoOCl_2]^+Cl^-$ is similar to that observed for $LMoOCl_2$.[15] Detailed interpretation of the electronic spectra of $LMoOX_2$ complexes is given elsewhere;[30] by analogy, the first and second bands of $[L^*MoOCl_2]^+Cl^-$ at 12 980 cm^{-1} ($\epsilon = 40$ M^{-1} cm^{-1}) and 27 700 cm^{-1} ($\epsilon = 1000$ M^{-1} cm^{-1}) are assigned as d → d transitions. The third band at 32 200 cm^{-1} ($\epsilon = 3200$ M^{-1} cm^{-1}) is assigned as a ligand to metal charge transfer transition. The unsymmetrical bis(μ-oxo) complexes both exhibit strong absorption in the visible region (≈25 000 cm^{-1}), probably due to a charge transfer transition involving the bridging oxo ligands.

Infrared Spectra. The infrared spectrum of $L^*Mo(CO)_3$ exhibits two v(CO) bands (Table 8) consistent with the $v_{sym}(A_1)$ and $v_{asym}(E)$ stretching modes in C_{3v} symmetry. Similar v(CO) stretching frequencies were observed for $[Et_4N][LMo(CO)_3]$[34] and $L'Mo(CO)_3$[14] complexes, indicating similar overall donor−acceptor properties for the three different ligands. The IR spectrum of L^*MoO_3 in the solid state shows three v(Mo═O) frequencies, indicating that the degeneracy of the E mode is lifted in L^*MoO_3. Similar behavior is observed in the $L'MoO_3$ (R = isopropyl)[13] complex.

The IR spectrum of $[L^*MoOCl_2]^+Cl^-$ shows a characteristic v(Mo═O) stretch at 979 cm^{-1}. The analogous $LMoOCl_2$ complex shows a v(Mo═O) stretch at 960 cm^{-1}, whereas $[L'MoOCl_2]^+[PF_6]^-$ shows a v(Mo═O) stretch at 970 cm^{-1}.

---

(27) Young, C. G.; Enemark, J. H. *Inorg. Chem.* **1985,** *24,* 4416.

(28) Minelli, M.; Enemark, J. H.; Brownlee, R. T. C.; O'Connor, M. J.; Wedd. A. G. *Coord. Chem. Rev.* **1985,** *68,* 169.

(29) Pauling, L. *J. Chem. Soc.* **1948,** 1461.

(30) Carducci, M. D.; Brown, C.; Solomon, E. I.; Enemark, J. H. *J. Am. Chem. Soc.* **1994,** *116,* 11856.

Table 7. Selected Bond Distances (Å) and Angles (deg) in $L^*Mo_2O_4(OC_6H_4O){\cdot}CH_3CN$

Distances			
Mo1−Mo2	2.5627(8)	Mo1−O1	1.686(5)
Mo1−O3	1.919(5)	Mo1−O4	1.919(5)
Mo1−O5	2.013(5)	Mo1−O6	2.006(5)
Mo2−O2	1.683(5)	Mo2−O3	1.924(5)
Mo2−O4	1.941(4)	Mo2−N11	2.217(6)
Mo2−N21	2.392(5)	Mo2−N31	2.230(6)
O5−C1	1.367(9)	O6−C6	1.346(9)
N11−N12	1.369(8)	N12−C10	1.445(9)
N21−N22	1.365(7)	N22−C10	1.446(9)
N31−N32	1.366(8)		

Angles			
O2−Mo2−N31	90.6(2)	O3−Mo2−O4	91.8(2)
O3−Mo2−N11	89.1(2)	O3−Mo2−N21	86.4(2)
O3−Mo2−N31	160.2(2)	O1−Mo1−O3	109.3(2)
O4−Mo2−N11	161.0(2)	O1−Mo1−O4	111.7(2)
O4−Mo2−N21	86.1(2)	O1−Mo1−O5	104.9(2)
O4−Mo2−N31	89.4(2)	O1−Mo1−O6	108.3(2)
O1−Mo1−O6	108.3(2)	N11−Mo2−N21	75.0(2)
O3−Mo1−O4	92.7(2)	N11−Mo2−N31	83.5(2)
O3−Mo1−O5	144.6(2)	N21−Mo2−N31	74.0(2)
O3−Mo1−O6	82.0(2)	Mo1−O3−Mo2	83.7(2)
O4−Mo1−O5	82.8(2)	Mo1−O4−Mo2	83.2(2)
O4−Mo1−O6	139.1(2)	Mo1−O5−C1	114.9(5)
O5−Mo1−O6	78.9(2)	Mo1−O6−C6	114.9(5)
O2−Mo2−O3	107.8(2)	Mo2−N21−N22	119.0(4)
O2−Mo2−O4	107.2(2)	O2−Mo2−N11	90.5(2)
O2−Mo2−N21	159.8(2)	Mo2−N31−N32	121.9(4)
N12−C10−N22	110.0(6)	N12−C10−N32	112.0(6)
N22−C10−N32	110.0(6)		

The unsymmetrical bis(μ-oxo) dimers $L^*Mo_2O_4Cl_2$ and $L^*Mo_2O_4(OC_6H_4O)$ exhibit infrared stretching frequencies in the 900−1000 and 750 cm^{-1} regions that are characteristic of the $[Mo_2O_4]^{2+}$ core.[24] In principle, two ν(Mo═O) frequencies should be observed for these asymmetric dimers. The very strong band in the 900−1000 cm^{-1} region is clearly one of these vibrations. The 23 cm^{-1} shift of this band between the two compounds implies that it is primarily centered on Mo1, whose coordination differs in the two compounds. One of the two medium-intensity bands in this region could be a ν(Mo═O) stretching frequency. However, ligand bands may also occur in this region.[31] Isotopic labeling experiments would be required to unambiguously assign the two medium-intensity bands in the 900−1000 cm^{-1} region. Both dimers exhibit $\nu(MoO_2Mo)$ stretching frequencies near 750 cm^{-1}.

EPR Spectra. The isotropic and anisotropic *g* values and the isotropic and anisotropic $^{95,97}Mo$ hyperfine parameters, *A*, for several molybdenum(V) species appear in Table 9. The frozen X-band EPR spectrum of $[L^*MoOCl_2]^+Cl^-$ is nearly axial and closely resembles the EPR spectrum of $LMoOCl_2$. The *g* and *A* parameters of $[L^*MoOCl_2]^+Cl^-$ were obtained by simulation (Table 9) and are similar to those for $LMoOCl_2$,[32,33] indicating that the EPR parameters are primarily governed by the local coordination environment at the molybdenum center. This similarity of EPR parameters for $LMoOCl_2$ and $[L^*MoOCl_2]^+$ extends to other analogous pairs of oxo−molybdenum(V) complexes of L and L*, and the solution formulations of the other complexes of L* shown in Scheme 2 are based upon the close similarity of their EPR parameters to those of analogous well-characterized molybdenum complexes of L.[15]

The fluid solution EPR spectrum for the proposed $[L^*MoO(catCl_4)]^+$ species in Scheme 2 shows $\langle g \rangle \approx 1.942$ and $\langle A \rangle = 42.33 \times 10^{-4}\ cm^{-1}$; the qualitative and quantitative similarity of its frozen solution EPR spectrum to that of the analogous $[LMoO(catCl_4)]$ complex supports the $[L^*MoO(catCl_4)]^+$ formulation. The fluid solution EPR spectrum of the reaction mixture containing $[L^*MoOCl_2]^+Cl^-$ and 1 equiv of $HSCH_2CH_2SH$ in the presence of base shows a signal at $\langle g \rangle \approx 1.980$, which is assigned to $[L^*MoO(SCH_2CH_2)]^+$. Addition of excess $HSCH_2CH_2SH$ to $[LMoOCl_2]^+Cl^-$ produces a single EPR-active species with $\langle g \rangle = 2.003$ and $\langle A \rangle = 29.76 \times 10^{-4}\ cm^{-1}$. The frozen solution EPR parameters obtained by simulation show nearly axial *g* and *A* values. The assignment of this species as $[MoO(SCH_2CH_2S)_2]^-$ was confirmed by comparing its EPR spectrum to that of an authentic sample of $[Et_4N][MoO(SCH_2CH_2S)_2]$.[18]

Electrochemistry. The redox properties of all mononuclear complexes have been examined by cyclic voltammetry in acetonitrile at 25 °C. All complexes exhibit pseudo-Nernstian one-electron redox couples as demonstrated by $i_{pa}/i_{pc} \approx 1$ (Table 10). The cyclic voltammogram of $L^*Mo(CO)_3$ in acetonitrile exhibits one quasi-reversible process at −0.234 V vs Fc^+/Fc ascribed to one-electron oxidation to the corresponding $[L^*Mo(CO)_3]^+$ species. Similar results have been reported for the electrochemistry of complexes of $L'Mo(CO)_3$[14] and $[LMo(CO)_3]^-$.[34] Cyclic voltammograms of the $LMoX_3$ complexes (X = Cl, Br, I) show a single one-electron oxidation process in the potential range between −1.5 to +1.5 V vs Ag/AgCl (eq 1). The redox potentials for these Mo(IV)/Mo(III)

$$[LMoX_3]^+ + e^- \rightleftharpoons [LMoX_3] \qquad X = Cl, Br, I \qquad (1)$$

couples are quite positive and span the relatively small range from +0.387 V (Cl^-) to +0.514 V (Br^-) vs the Fc^+/Fc couple. The order of increasing positive redox potentials as a function of X^- is $I^- \approx Br^- > Cl^-$. Thus, the Mo(IV) oxidation state is more stabilized by the small chloride ligand than the bulky more polarizable bromide and iodide ligands. These potentials are very similar to those observed for $L'MoX_3$ complexes[14] (X = Cl, Br, I). The electrochemical behavior of $L'MoX_3$ and L^*MoX_3 complexes contrasts with that of anionic $[LMoCl_3]^-$ complex, where two one-electron oxidations are observed.[22,35] The close similarity of the Mo(IV/III) couples for $L'MoX_3$ and L^*MoX_3 (aliphatic and aromatic nitrogen donor atoms, respectively) implies that the π-acceptor ability of these neutral tridentate ligands is not a major factor in the stability of these complexes.

The cyclic voltammogram of $[L^*MoOCl_2]^+Cl^-$ in acetonitrile exhibited a pseudoreversible one-electron reduction at −0.300 V. Similar reduction processes are observed for $LMoOCl_2$ (−0.739 V) and $[L'MoOCl_2]^+$ (−0.520 V) complexes (Table 10). The L* ligand stabilizes the oxo−Mo(IV) state more than analogous L and L′ ligands. However, $L^*Mo^{IV}OCl_2$ is still too easily oxidized to be useful as a possible diamagnetic host for $LMo^{V}OCl_2$, one of the original goals of this research.

Summary. This investigation is the first study of molybdenum complexes of L*. The molybdenum(0 and III) chemistry of this ligand parallels that of the analogous complexes of L and L′, whereas the oxomolybdenum chemistry of L* exhibits significant differences from that of L and L′. The attempts to

---

(31) Desrochers, P. J.; Nebesny, K. W.; LaBarre, M. J.; Bruck, M. A.; Neilson, G. F.; Sperline, R. P.; Enemark, J. H.; Backes, G.; Wieghardt, K. *Inorg. Chem.* **1994,** *33,* 15.

(32) Collison, D.; Eardley, D. R.; Mabbs, F. E.; Rigby, K.; Enemark, J. H *Polyhedron* **1989,** *8,* 1833.

(33) Collison, D.; Eardley, D. R.; Mabbs, F. E.; Rigby, K.; Bruck, M. A.; Enemark, J. H.; Wexler, P. A. *J. Chem. Soc., Dalton Trans.* **1994,** 1003.

(34) Trofimenko, S. *J. Am. Chem. Soc.* **1969,** *91,* 588.

(35) Direct comparison of the redox potentials of L^*MoX_3 complexes with $[LMoCl_3]^-$ is not possible because the latter data were not internally referenced to the Fc^+/Fc system.

Table 8. UV−Visible and IR Data

complex	UV−vis: E_{max} (10^3 cm^{-1}) (ϵ (10^3 L mol^{-1} cm^{-1}))[a]	IR (cm^{-1})[b]
[L*Mo(CO)$_3$]	*c*	v(CO) 1900, 1763
[L*MoCl$_3$]	12.97 (0.048), 28.24 (1.07), 34.72 (3.12), 45.57 (22.17)	
[L*MoBr$_3$]	14.08 (0.007), 22.78 (0.833), 36.23 (14.23), 47.17 (26.53)	
[L*MoI$_3$]	13.35 (0.081), 24.63 (6.77), 30.86 (10.50)	
[L*MoO$_3$]	*c*	v(Mo=O) 898, 863, 840
[L*MoOCl$_2$]$^+$Cl$^-$	12.98 (0.04), 27.7 (1.68), 32.2 (3.2)	v(Mo=O) 979
[L*Mo$_2$O$_4$Cl$_2$]	24.75 (0.425), 31.84 (4.39), 45.24 (20.5)	v(Mo=O) 918, 945, 984; v(MoO$_2$Mo) 742
[L*Mo$_2$O$_4$(OC$_6$H$_4$O)]	26.11 (1.23), 33.44 (11.34), 47.17 (48.88)	v(Mo=O) 914, 940, 959; v(MoO$_2$Mo) 750

[a] In acetonitrile. [b] KBr pellet. [c] Not soluble.

Table 9. EPR Data

complex	g_1	g_2	g_3	$\langle g \rangle$	A_1[a]	A_2	A_3	$\langle A \rangle$	α[b]	β[b]	γ[b]	ref
LMoOCl$_2$	1.971	1.941	1.934	1.948	71.40	18.10	38.10	42.53	0	33	0	32
[L*MoOCl$_2$]$^+$Cl$^-$	1.976	1.949	1.934	1.953	73.38	21.34	40.02	44.91	0	38	0	this work
LMoO(catCl$_4$)[c]	1.969	1.967	1.927	1.955	32.02	18.01	68.38	39.47	0	31	30	17
[L*MoO(catCl$_4$)]$^+$	1.956	1.955	1.926	1.942				42.33				this work
[MoO(SCH$_2$CH$_2$S)$_2$]$^-$[d]	2.012	1.997	1.975	1.999				30.30				18
[MoO(SCH$_2$CH$_2$S)$_2$]$^-$[e]	2.052	1.983	1.979	2.003	49.40	18.67	20.72	29.76	0	0	0	This work

[a] $A(^{95,97}$Mo) × (10^{-4} cm^{-1}). [b] α, β, and γ (deg) are Euler angles. [c] catCl$_4$ = 2,3,4,5-tetrachlorocatecholate. [d] EPR parameters obtained directly from spectrum without simulation. [e] Compound synthesized by literature method.[18] The EPR spectrum is identical to that shown in ref 18; EPR parameters obtained by simulation.

Table 10. Electrochemical Data[a−c]

couple	complex	E_f (V) (ΔE_p (mV))	i_{pa}/i_{pc}
Mo(I/0)	[LMo(CO)$_3$]$^{0/-}$	−0.501(79)	1.0
Mo(I/0)	[L*Mo(CO)$_3$]$^{+/0}$	−0.234(72)	1.1
Mo(I/0)	[L′Mo(CO)$_3$]$^{+/0}$	−0.245(68)	d
Mo(IV/III)	[L*MoCl$_3$]$^{+/0}$	0.387(64)	1.0
Mo(IV/III)	[L′MoCl$_3$]$^{+/0}$	0.395(65)	0.8
Mo(IV/III)	[L*MoBr$_3$]$^{+/0}$	0.514(58)	1.0
Mo(IV/III)	[L′MoBr$_3$]$^{+/0}$	0.500(72)	0.9
Mo(IV/III)	[L*MoI$_3$]$^{+/0}$	0.508(57)	*d*
Mo(IV/III)	[L′MoI$_3$]$^{+/0}$	0.525(65)	*d*
Mo(V/IV)	[LMoOCl$_2$]$^{0/-}$	−0.739(72)	0.9
Mo(V/IV)	[L*MoOCl$_2$]$^{+/0}$	−0.300(64)	1.1
Mo(V/IV)	[L′MoOCl$_2$]$^{+/0}$	−0.520(65)	1.0

[a] Conditions: cyclic voltammetry, Pt electrode, 1−2 mM solutions in CH$_3$CN, 0.1 M Me$_4$NPF$_6$ for L and L* complexes. [b] Potentials vs Fc$^+$/Fc, 23 °C. [c] For L′ complexes see ref 14. [d] Dependent on scan rate.

synthesize neutral L*Mo^{IV}OX$_2$ complexes were not realized because of the facile oxidation of such species to cationic oxo−Mo(V) species, such as [LMoOCl$_2$]$^+$Cl$^-$. An unusual feature of the oxo−Mo chemistry of L* is the unexpected lability of the ligand as evidenced by the formation of unsymmetrical bis-(μ-oxo) dimers, such as [L*Mo$_2$O$_4$Cl$_2$], and complete replacement of L* by $^-$SCH$_2$CH$_2$S$^-$ in basic solution to produce [Mo^{V}O(SCH$_2$CH$_2$S)$_2$]$^-$. The unexpected lability of [L*Mo^{V}OX$_2$]$^+$ complexes cannot be due to differences in steric or electronic requirements of L and L* because the structural parameters of the two ligands are nearly identical and the electronic and EPR spectra of LMo^{V}OCl$_2$ and [L*Mo^{V}OCl$_2$]$^+$ are very similar. The positive charge on [L*Mo^{V}OCl$_2$]$^+$ and its derivatives may be the reason for their enhanced substitution reactivity with anionic ligands compared to that of LMo^{V}OX$_2$ complexes. The improved synthetic route to L* [7] and the range of chemistry observed for L* in this restricted study provide encouragement for investigations of the coordination chemistry of this ligand with other metals.

Acknowledgment. We thank Prof. Belford and co-workers for making the program QPOW available to us, Dr. Arnold Raitsimring for measuring the EPR spectra, Dr. Roger Sperline for measuring the FT-IR spectra, Dr. Kenner Christensen for recording the ^{95}Mo NMR spectra, and Dr. Michael Carducci for helpful discussions. Financial support from the National Institutes of Health (Grant GM-37773) and National Science Foundation (Grant DIR-9016385 for the EPR spectrometer) is gratefully acknowledged. B.S. thanks the National Science Foundation for a summer fellowship through the REU program. The X-ray structure determinations were carried out in the Molecular Structure Laboratory of the University of Arizona.

Supporting Information Available: Tables of crystallographic details, anisotropic thermal parameters, calculated hydrogen atomic positions, and bond distances and angles for L*MoI$_3$, L*Mo$_2$O$_4$Cl$_2$, and L*Mo$_2$O$_4$(OC$_6$H$_4$O) complexes (17 pages). Ordering information is given on any current masthead page.

IC950078U